KKU Engineering Journal

https://www.tci-thaijo.org/index.php/easr/index

Published by the Faculty of Engineering, Khon Kaen University, Thailand

Filtration efficiency and filter resistance of nylon-6 and nylon-6/chitosan nanofibrous membranes

Panu Danwanichakul*, Duangkamol Danwanichakul, Adisara Yooyanyong and Kantika Sae-Ieo

Department of Chemical Engineering, Faculty of Engineering, Thammasat University, Pathumthani 12120, Thailand

Received June 2015
Accepted August 2015

Abstract

Pore size reduction of nanofibrous membranes and the removal efficiencies for submicron PS particles (410, 200, 90 and 50 nm) were investigated in this study. Blending chitosan with nylon-6 generated ultrafine fibers among typical nanofibers produced an electrospun membrane with a smaller average pore size. It was found that high molecular weight chitosan could increase the filtration efficiency to a greater degree than low molecular weight chitosan. The best membrane was obtained from a solution of 30% wt/v nylon-6 and 0.06% wt/v chitosan. It had an average fiber size of around 128 nm, average pore size of 110 nm and a thickness of 0.1 mm. While it could completely remove larger particles, it gave a removal efficiency of 94% for 50-nm particles when it was used as a single-layer membrane and up to 97% as a double-layer of membranes with an overall thickness of 0.17 mm. It had a greater removal efficiency than a commercial nylon membrane and smaller pore sizes. Therefore, it has a potential to be used for sterilization of contaminated water.

Keywords: Filtration, Nanoparticles, Nanofibers, Electrospinning, Nylon, Chitosan

1. Introduction

Electrospinning, which is one of several methods producing sub-micron scale fibers, has been increasingly investigated due to its low cost, simplicity and controllability. So far, more than 200 polymers have been electrospun and studied for many applications among which is the membrane filtration [1]. The network of deposited nonwoven nanofibers of the filter generates submicron connecting pores resulting in high performance in capturing submicron particles [2]. This application is so important in purification of water and air that a large number of results have been reported in the literature.

For example, the electrospun polyvinylidene fluoride membranes were investigated for the separation of polystyrene micro-particles in liquid phase. With thickness of 0.3 mm and pore size ranging from 4 to 10 μm, the membrane could reject 90% of particles [3]. Electrospun polyacrylonitrile nanofibers were also applied as a midlayer support in membranes for ultrafiltration of $MgSO_4$ particles in water [4]. In addition, electrospun nylon-6 fibrous membrane has been prepared and employed as a membrane material without any treatment for water filtration due to its excellent chemical and thermal resistance as well as its high wettability. Due to high wettability of nylon, it should gain more interest regarding high flux of water and low possibility of fouling.

Nylon-6 nanofibers could be utilized effectively as a pre-filter for removal of micron and sub-micron particles. The removal efficiency could be up to 85 to 100% depending on the relative sizes of pores and particles [5]. In addition, nylon-6 nanofibrous membranes were also employed to remove aerosols, where the Peclet number and slip flow phenomena were investigated along with the filtration efficiency [2]. Besides the high flux and selectivity, the aim of filtration is also focused on efficient removal of nano-particles. The removal of particles as small as 50 nm is a challenge and it could find applications in separation of some metal nanoparticles after synthesis and in removal of certain bacteria and viruses. This is necessary in sample preparation before testing with high performance liquid chromatography (HPLC). It was reported experimentally and theoretically that the pore size of nanofibrous structures depended on the size of nanofibers given that the membrane was thick enough [6]. Therefore, a method to reduce pore size is producing fibers as small as possible by lowering the concentration of nylon-6 solution [7]. Another interesting method is by producing the biomodal nanofibers which could yield higher filtration efficiency than unimodal nanofibers [8].

It has been reported that incorporating other materials in nylon-6 solutions could generate bimodal nanofibers upon electrospinning. Pant *et al.* successfully prepared the spider-net like nanofiber mat containing TiO_2 nanoparticles [9]. Nirmala *et al.* also successfully obtained similar nanofibrous structures when electrospinning the solution of nylon-6 blended with chitosan [10]. The latter system was investigated for biomedical applications owing to the attractive properties of chitosan such as antibacterial and antifungal activity, non-toxicity, biodegradability and biocompatibility. However, only few works have discussed

*Corresponding author. Tel.: +66 2564 3001 ext.3123; fax: +66 2564 3024
Email address: dpanu@engr.tu.ac.th
doi: 10.14456/kkuenj.2016.5

the system of nylon-6/chitosan blend. Nylon-6/chitosan nanofibrous filter media could offer the distinct advantages of pore size and chemistry of fibers to achieve desired filtration properties compared to nanofibrous filter media fabricated from other synthetic polymers.

In this research, the blend system of nylon-6/chitosan nanofibers is, thus, investigated for its filtration performance, which has not been reported before. The ratio of nylon-6 and chitosan was adjusted to obtain the nanofibrous membrane with the small average fiber size. Two molecular weights of chitosan were investigated as a factor influencing the formation of ultrafine fiber. The obtained mat was expected to have good removal efficiency for particles as small as 50 nm. The comparison between the obtained mat and the commercial nylon membrane was also made.

2. Research methodology

2.1 Material

High molecular weight chitosan (CS) (Mw > $1x10^6$ and %DD of 98.6) was obtained from A.N. Lab Aquatic Nutrition, Thailand and low molecular weight chitosan (COS) (Mw about 300,000) was from the modification of CS following the method of Chuachamsai *et al.* [11] Nylon-6 was purchased from Sigma-Aldrich Co. LLC. Formic acid was supplied by Ajax Finechem Pty Ltd. The suspensions of polystyrene particles with average particle sizes of 90 nm (50-100 nm), 200 nm (200-300 nm) and 410 nm (400-600 nm) were purchased from Spherotech, Inc. The suspension of monodispersed polystyrene (PS) particles with an average particle size of 50 nm (49-51 nm) was obtained from Microspheres-Nanospheres, Inc. The commercial nylon membrane filter (Whatman™) available in the market has the reported average pore size of 0.2 µm, the diameter of 13 mm, and the thickness of 0.15 mm. It was produced via phase inversion method.

2.2. Polymer solution preparation

To prepare 30%w/v nylon-6 (N30) solution, 3 g of nylon-6 was dissolved in 10 ml of 90 wt% formic acid solution. For preparing N30/CS2 or N30/COS2 solution, 3 g of nylon-6 was firstly dissolved in 10 ml of formic acid and 0.06 g of chitosan, equivalent to 2% of nylon content, was added later into the solution. After that, the solution was mixed by a magnetic stirrer until it was homogenous. Other spinning solutions were prepared in the similar way.

2.3. Electrospinning process

Nylon-6 nanofibers and nylon-6/CS nanofibers were produced by electrospinning technique. In the experiment, 21 kV was generated by a high voltage power supply. The electrode was connected to the metal needle (No. 21G) of a syringe while the ground was connected to the stationary collector covered with a 3.5 x 3.5 cm^2 copper plate. The distance between the tip and the collector was fixed at 9 cm. The electrospinning time was varied in order to obtain membranes with thickness around 0.075, 0.10 and 0.17 mm.

2.4 Nanofiber characterization

Morphology of nanofibers was observed by using scanning electron microscopy (SEM) (Hitachi, modelS-3400N). The average diameter of electrospun nanofibers and the apparent average pore size of the structures were measured with an image analyzer. The apparent average pore size can be obtained by adjusting the contrast of the figure to yield the apparent fiber coverage of 0.28. (The coverage is the fraction of area covered by deposited fibers.) This value was chosen since it gave the results similar to the ones from the method in section 2.5. After that, the pore size could be estimated from a square root of the pore area. A digital micrometer thickness gauge was used to measure the thickness of nanofiber mats.

2.5 The average pore size determination by Hagen-Poiseuille equation

In this experiment, a syringe containing 5 ml water was vertically connected to a filter holder where the filter medium would be placed inside. A 0.5 kg piece of metal was then placed at the end of the syringe pushing the water through the filter medium. The volumetric flow rate of water was measured. The flow is so slow that it could be considered a laminar flow and pores inside nanofibrous structure are usually interconnected, thus the structures resemble a bundle of tortuous tubes. To simplify the calculation, the tortuosity was neglected and the Hagen-Poiseuille equation should be applied. In this research, the Reynolds number (*Re*) was $7.41x10^{-5}$±$1.05x10^{-5}$ which ensured the flow to be laminar. Therefore, the approximate average pore diameter of nanofibrous structures can be determined by Hagen-Poiseuille equation [12],

$$\frac{d^2}{32} = \frac{u\mu z}{\Delta P} \tag{1}$$

Where, d is the volume-average pore diameter (m), u is the velocity (m/s), μ is the viscosity of water at 25°C (Pa·s), z is the filter medium thickness (m) and ΔP is the pressure drop (Pa).

2.6 Filtration of polystyrene particles

First, 5 %w/v polystyrene particle suspensions of 90-nm, 200-nm and 410-nm PS particles were diluted to obtain a lower concentration of 200 ppm. For 50-nm PS particles, the suspensions were prepared by diluting 2.5% w/v to obtain 200 ppm and 400 ppm suspensions. After that, a membrane was put into a filter holder with a diameter of 13 mm. PS particle suspension in 5-ml syringe was pumped by a syringe pump at a constant flow rate of 8 µl/sec. The PS concentration of the filtrate was determined by comparing with the calibration curve. Spectrophotometer at 326 nm and 490 nm was used to measure the absorbance of the filtrates of 50-nm PS particles and larger particles, respectively. The filtration results were compared with those using Whatman™ nylon filter membrane. In this study, membrane thickness ranged from 0.075 to 0.17 mm. Several types of nanofibrous membranes including 30 %w/v pure nylon-6 (N30), 30 %w/v nylon-6 blended with 0.3 %w/v and 0.6 %w/v chitosan (N30/CS2) and 30 %w/v nylon-6 blended with 0.6 %w/v chito-oligosaccharides (N30/COS2) were studied and compared with the commercial membrane. All membranes were used only once except for the repetition test of filtration cycles in which a membrane was used up to 14 times. The removal efficiency was determined by using the equation below.

$$Removal\ Efficiency\ (\%) = \left(1 - \frac{C_{filtrate}}{C_{initial}}\right) x100 \tag{2}$$

Where, $C_{filtrate}$ and $C_{initial}$ are PS particle concentrations in the filtrate and in the feed, respectively.

3. Results and discussion

This part shows the results and discussion about PS particles filtration by the obtained electrospun membranes. The discussion is given for three factors which are membrane thickness, filter material type and the repetition of filtration cycles of a membrane.

Considering the formation of PS particle cake at the front of the filter medium during filtration and applying Bernoulli's equation over the plane of PS-particle cake surface to the back of the medium where the filtrate comes out with the assumption that the pressure drop across both surfaces, (P_1-P_3), is constant, a differential equation regarding the volume of the filtrate (V) and the filtration time (t) could be derived and finally integrated to obtain [13]

$$t = \frac{\mu w}{2KA^2}\frac{1}{(P_1 - P_3)}V^2 + \frac{\mu a}{A(P_1 - P_3)}V \qquad (3)$$

Where, w is the ratio between cake volume and filtrate volume, μ is viscosity of liquid, K is the permeability of the cake, A is the surface area of the medium, and a is the medium resistance which is equal to the ratio of the medium thickness, x, and the permeability of the medium itself. In the case that cake filtration is neglected at the beginning of filtration process, P_2, which is the pressure at the interface of cake and medium, could be approximately equal to P_1.

In this work, the syringe pump was used during filtration so the pressure drop could be considered constant so equation (3) should be applied. Considering the result of every case, it was found that the coefficient in front of V^2, which represents the resistance of the formed cake, was negligible when compared with the coefficient in front of V, which represents the resistance of the filter medium, implying that the effect of cake is not significant in this case due to low concentration of PS particles in the suspension. The discussion about the resistance in filtration, therefore, follows the linear fitting of the experimental data, V and t. The slope of the graph relates to the resistance of the medium, a, as mentioned above and is in fact $1/Q$, where Q is the volumetric flow rate.

3.1. Effect of membrane thickness

Figure 1 shows morphology and size distribution of nanofibers at the front of the membrane produced from N30 solution with different thickness ranging from 0.074 to 0.168 mm. The fiber size of the sample with thickness of 0.074 mm (Figure 1(b)) ranged between 80 to 270 nm, that of sample with thickness of 0.10 mm (Figure 1(d)) ranged between 100 to 250 nm and that of sample with thickness of 0.168 mm ranged between 80 and 550 nm among which a few large fibers are seen in Figure 1(f).

In theory, the average size and size distribution should be the same regardless of the membrane thickness. In reality, the mixing of solution had to be done very carefully to assure homogeneity of the solution since local viscosity in solution may produce the fibers with obviously different diameters.

Figure 2(a) shows the fiber and pore sizes obtained both from SEM and Hagen-Poiseuille's equation. In an image analysis of the SEM figure, it certainly depends on the judgment of the researcher to measure the pore size generated by deposition of many layers of fibers. Therefore, the results were compared first when adjusting the contrast

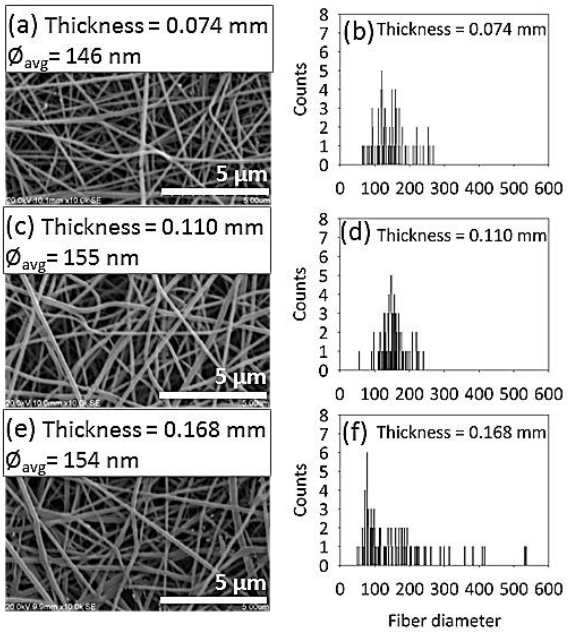

Figure 1 Morphology and size distribution of N30 membrane with different thickness

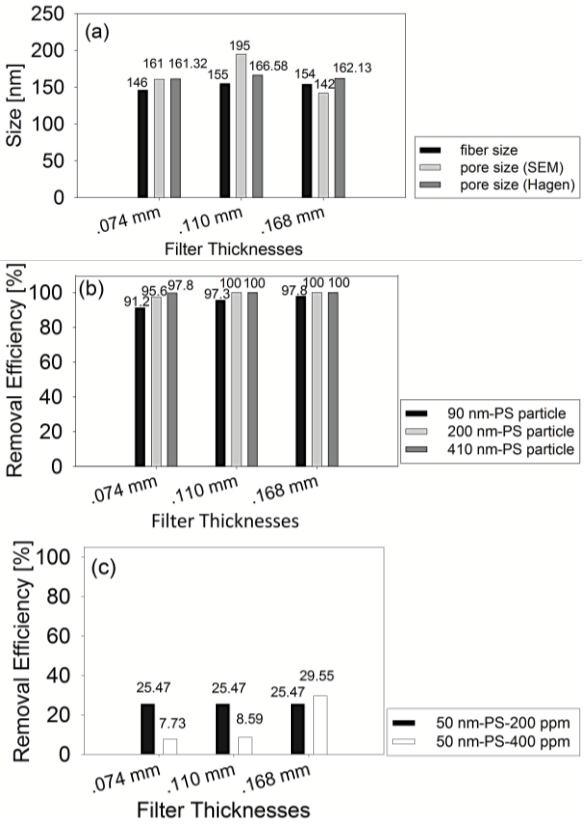

Figure 2 Fiber size, pore size and removal efficiency of N30 membrane with different thicknesses

of the SEM figure, thereby changing the surface coverage of the fibers. It was found that results from SEM figures were most consistent to the ones from Hagen-Poiseuille's equation when the fiber coverage was about 0.28. So this process was adopted in the measurement of the pore size from SEM figures.

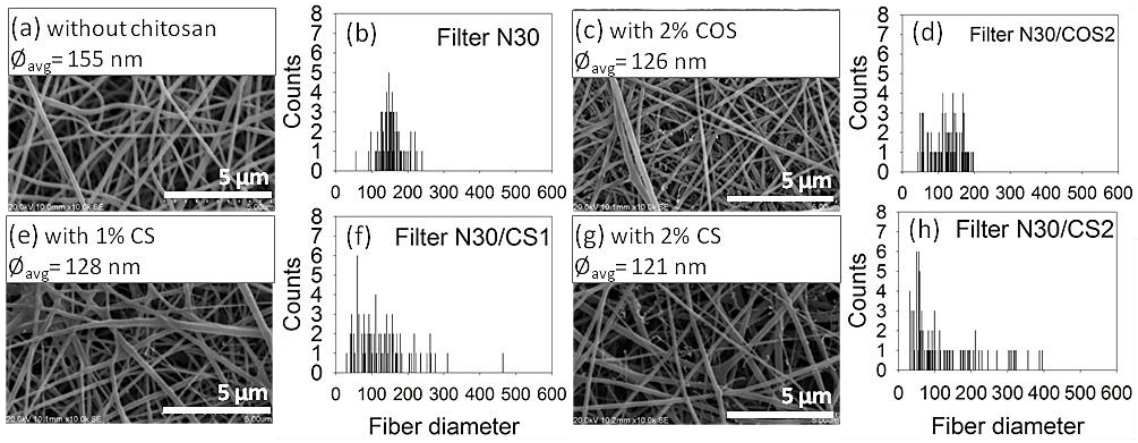

Figure 3 Morphology and size distribution of nanofibers with thickness of 0.10

It can be seen from Figure 2 that fiber sizes were around 150 nm and pore sizes were less than 200 nm. Especially, the volume-averaged pore sizes from flow measurement and Hagen-Poiseuille's equation of all samples were almost the same around 165 nm. So when spinning a thicker membrane, the morphology of the fiber was safely assumed unchanged and the fiber sizes and pore sizes were in around the same range.

The filtration performance of N30 nanofibrous membranes with different thickness from 0.074 to 0.168 mm to remove 90-nm, 200-nm and 410-nm PS particles is reported in terms of %removal efficiency as shown in Figure 2(b) as well as the filtration performance for 50-nm PS particles in Figure 2(c). It was found that a thicker membrane had a higher efficiency as reported by Aussawasathien *et al* [5]. The thicker membrane completely removed the larger particles (200 nm and 410 nm), which was attributable to the relative sizes of the pore and the particle, i.e. particles larger than 165 nm, the average pore size, should be effectively removed from the suspension. But the incomplete removal was seen for the case of 0.074 mm-thick membrane possibly because the membrane was too thin and its nanofibers could be broken when large particles attempted to pass through. On the contrary, the removal efficiency dropped dramatically when fine particles (50 nm) were filtered with all membranes as displayed in Figure 2(c).

3.2 Effect of filter material

To increase the removal efficiency of the membranes studied in the previous section, the formation of ultrafine fibers were investigated by blending nylon-6 and high molecular weight chitosan (CS) or nylon-6 and low molecular weight chitosan (COS). Figure 3 shows the morphology of nanofibers with and without chitosan along with their fiber size distribution. It was seen that ultrafine nanofibers were produced from the blend of nylon-6 and chitosan as reported by Nirmala *et al.* [10]. It is shown in this study that either blending CS or COS at the same chitosan content could yield the same average fiber diameter but, with CS, the fiber size distribution shows a population of larger fibers. In addition, increasing chitosan content could generate more ultrafine fibers. As discussed by Zhang *et al*. [14], it was expected that the formation of hydrogen bonding between chitosan and nylon-6 molecules in such system should be responsible for the heterogeneity of the solution in which there might be regions with different local viscosity and conductivity, resulting in formation of ultrafine fibers among typical ones.

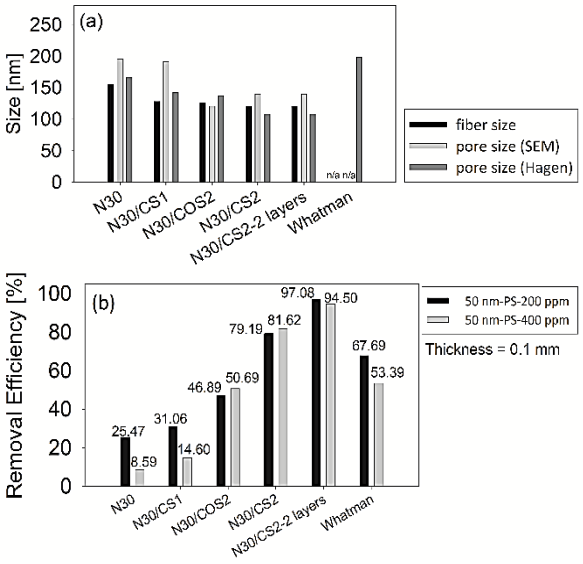

Figure 4 Fiber size, pore size and removal efficiencies of membrane for 50-nm particles

Figure 4(a) compares the fiber size and pore size of membranes from different polymer systems. For the commercial membrane (Whatman^{TM}), the pore size obtained from Hagen-Poiseuille's equation was 198 nm which is close to the reported value of 200 nm from the company. Apparently, our produced membranes have smaller pores than the commercial one.

When tested, commercial membranes could remove 200-nm and 410-nm PS particles from the 200-ppm suspension completely but it could remove only 5.6 % of 90-nm PS particles because PS particles were much smaller than its pore size. Confronting this challenge of removing 50-nm PS particles, all produced nanofibrous membranes were tested along with the commercial one. The membranes of nylon-6 and CS could remove PS-particles better than the sample with COS as can be seen in Figure 4(b). This is probably because high molecular-weight chitosan is less miscible with nylon-6 resulting in creation of more heterogeneous structure containing more ultrafine fibers. The morphology is shown in Figure 5, in which a larger number of small particles were captured on the front surface of samples with CS than with COS and without chitosan at all. Despite the obvious formation of ultrafine fibers, we should not leave out the influence of hydrophilicity of the fiber surface, which should be investigated in more detail.

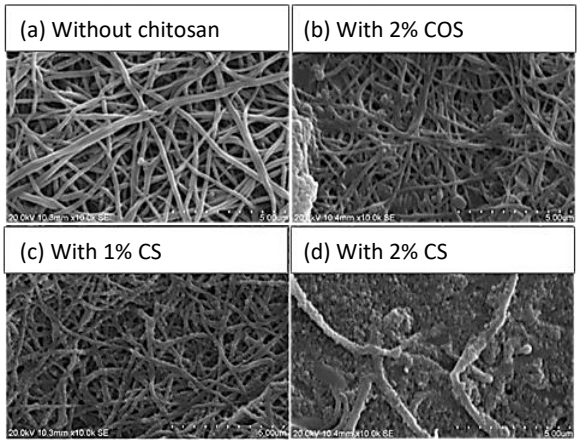

Figure 5 Morphology at the front of N30/chitosan membranes with thickness of 0.100 mm, after filtration of PS particles

In addition, to further increase the filtration performance of nylon-6 blended with chitosan membranes, the double-layer membranes were applied. They were actually two separate membranes packed side by side in the same holder to make a total thickness of 0.17 mm. The removal efficiencies for 50-nm PS particles in the suspension of 200 and 400 ppm were increased from 79.19% to 97.08% and 81.62% to 94.50% respectively when the double layers were used instead of the single layer. The single-layer commercial membrane (Whatman^{TM}) gave the removal efficiency as high as 67.69 % and 53.39% for 50-nm PS particles with concentration 200 ppm and 400 ppm, respectively. The results were better than when it was used to remove 90-nm particles probably because of the higher degree of aggregation of smaller particles.

The morphology of the commercial nylon membrane is presented in Figure 6. It is obvious that PS particles with diameters of 50 and 90 nm were not much seen on the membrane indicating that they could pass through the membrane pores. Unlike those smaller particles, 200-nm particles could aggregate and form continuous cake on the surface and 400-nm particles could also block the surface pores and stayed on the membrane front. Considering these comparative results, our produced membrane can probably be used to remove nano-scale particles down to 50 nm such as flu virus and bacteria.

The resistance during filtration could also be interpreted from the filtration results for all these membranes. Figure 7 compares the filter resistance which is related to $1/Q$. It is seen that our membranes gave higher $1/Q$ than the commercial membrane (Whatman^{TM}), implying the better performance for filtration as discussed earlier. These values conform to the data of membrane pore size (Figure 4(a)) as well as the removal efficiency of PS particles (Figure 4(b)). It should also be noted that from Figure 4, N30 membrane had smaller pores but it could remove 50-nm particles with lower efficiency than Whatman^{TM} membrane. It is possible that the structure inside the membrane might play a role. The electrospun membrane is known for its pore-interconnectivity so particles might have a fewer chance to block the vacant path inside the membrane than inside Whatman^{TM} membrane.

3.3. Repetition of filtration cycles

Since we expected that some nanofibers might be easily broken during the filtration process, to test the repetition of filtration cycles, we used the worst case scenario where the most fragile fibers with unimodal size distribution were obtained from N25 solution (which has not been discussed so far) and PS particles were of the largest size, 410 nm. The fiber average size was only 120 nm so the removal efficiency for 200-ppm suspension was expected to be high. The filtration of the N25 membrane was successively repeated for 14 times, each with 5 ml suspension. It was found that only in the first trial the removal efficiency was 27.93%. From the second to fourteenth trials the removal efficiency reached 100%. The accumulating cake formed during successive filtration seemed to facilitate the removal of PS particles and it was found that the slope between the filtrate volume and time (equivalent to $1/Q$) did not change during the repetition test, implying that the cake did not contribute much to the filtration resistance which confirms the assumption of linear behavior of simplified version of equation (3). This is such the case. As the cake forms in two-dimensional space, the

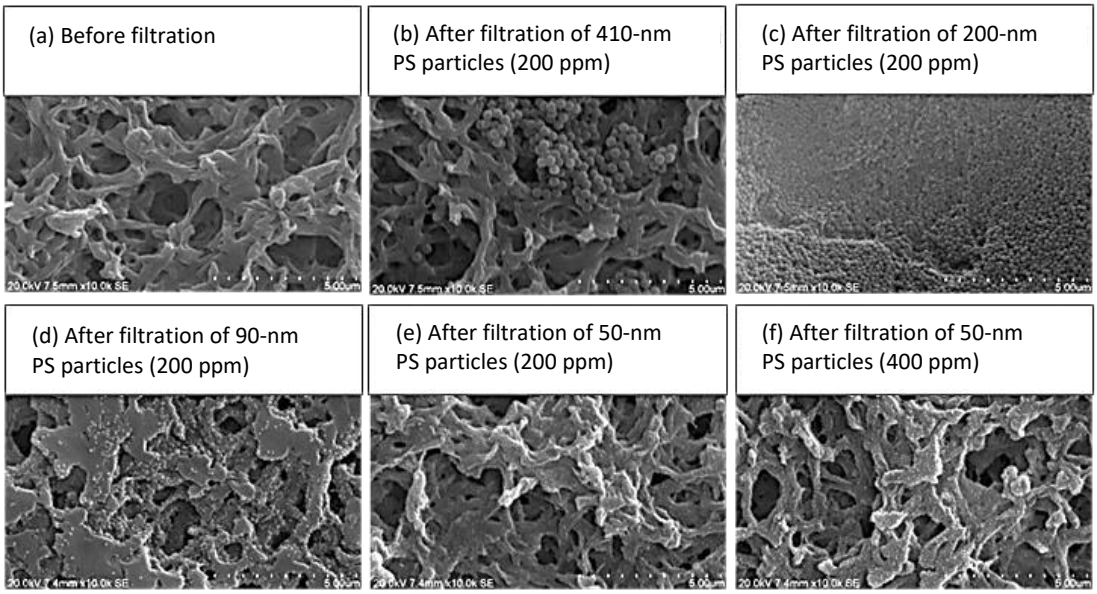

Figure 6 Morphology of the front of the commercial nylon membranes before and after filtration of PS particles

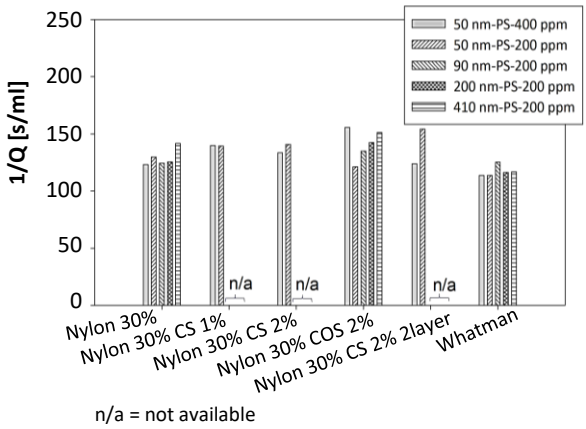

Figure 7 Filter resistance in filtration of various membranes

packing of spherical particles is of hexagonal arrangement where the generated pores have the size around half of a particle diameter, which is around or less than 200 nm. The average size of N25 nanofibers is still smaller so the pores of the cake should not contribute to the filtration resistance but the cake could strengthen the membrane and in some degree prevent the breakage of fine nanofibers. However, we should expect different result in the experiment with a thick cake formed by fine particles where the pore size of the cake is less than the pore size of the nanofibrous structures.

4. Conclusions

Many factors influencing the filter performance in filtration of submicron down to 50-nm colloidal particles using nanofibers were investigated. Normally, the main factors governing efficiency are cake resistance and membrane resistance. In this research, cake resistance could be negligible because only very thin cakes were formed. (Both the volume and concentration of suspension to be tested were small.) It could be concluded that blending chitosan with nylon-6 is essential in this study because the ultrafine fibers were generated among typical nanofibers. However, the optimum thickness for a particular membrane has to be determined in order to maximize the mechanical strength and removal efficiency and at the same time minimize the cost of production.

5. Acknowledgments

This research was financially supported by Thammasat University for the fiscal year 2013.

6. References

[1] Choi H, Kim SB, Kim SH, Lee M. Preparation of electrospun polyurethane filter media and their collection mechanisms for ultrafine particles. J Air Waste Manage. 2014; 64(3):322-9.

[2] Zhang S, Shim WS, Kim J. Design of ultra-fine nonwovens via electrospinning of Nylon 6: Spinning parameters and filtration efficiency. Mater Design. 2009;30(9):3659-66.

[3] Gopal R, Kaur S, Ma Z, Chan C, Ramakrishna S, Matsuura T. Electrospun nanofibrous filtration membrane. J Membrane Sci. 2006;281(1-2):581-6.

[4] Yoon K, Hsiao BS, Chu B. High flux ultrafiltration nanofibrous membranes based on polyacrylonitrile electrospun scaffolds and crosslinked polyvinyl alcohol coating. J Membrane Sci. 2009;338:145-52.

[5] Aussawasathien D, Teerawattananon C, Vongachariya A. Separation of micron to sub-micron particles from water: electrospun nylon-6 nanofibrous membranes as pre-filters. J Membrane Sci. 2008;315(1-2): 11-9.

[6] Danwanichakul P, Danwanichakul D. Two-dimensional simulation of electrospun nanofibrous structures: connection of experimental and simulated results. J Chem. 2014;2014:1-10.

[7] Noorpoor AR, Sadighzadeh A, Anvari A. Effect of Nylon-6 Concentration on Morphology and Efficiency of Nanofibrous Media. Int J Environ Res. 2014;8(2):421-6.

[8] Mei Y, Wang Z, Li X. Improving filtration performance of electrospun nanofiber mats by a bimodal method. J Appl Polym Sci. 2013;128(2):1089-94.

[9] Pant HR, Bajgai MP, Nam KT, Seo YA, Pandeya DR, Hong ST, Kim HY. Electrospun nylon-6 spider-net like nanofiber mat containing TiO(2) nanoparticles: a multifunctional nanocomposite textile material. J Hazard Mater. 2011;185(1):124-30.

[10] Nirmala R, Navamathavan R, Kang HS, El-Newehy MH, Kim HY. Preparation of polyamide-6/chitosan composite nanofibers by a single solvent system via electrospinning for biomedical applications. Colloid Surface B. 2011;83:173-8.

[11] Chuachamsai A, Lertviriyasawat S, Danwanichakul P. Spinnability and defect formation of chitosan/poly vinyl alcohol electrospun nanofibers. Thammasat Int J Sci Tech. 2008; 13:24-9.

[12] Johnston PR. Fluid sterilization by filtration. 3rd ed. Boca Raton: Interpharm/CRC; 2003.

[13] de Nevers N. Fluid mechanics for chemical engineers. 2nd ed. New Jersey: McGraw Hill. Inc; 1991.

[14] Zhang H, Li S, Branford WCJ, Ning X, Nie H, Zhu L. Studies on electrospun nylon-6/chitosan complex nanofiber interactions. Electrochim Acta. 2009; 54(24):5739-45.